FEMORAL STRENGTH PREDICTION USING A 3D RECONSTRUCTION METHOD FROM DUAL-ENERGY X-RAY ABSORPTIOMETRY

Ludovic Humbert[2,1], Tristan Whitmarsh[1,2], Karl Fritscher[3], Luis Miguel del Río Barquero[4], Felix Eckstein[6], Thomas Link[7], Rainer Schubert[3], Alejandro F. Frangi[1,2,8]

[1] Computational Imaging and Simulation Technologies in Biomedicine, Universitat Pompeu Fabra, Barcelona, Spain
[2] Networking Biomedical Research Center - Bioengineering, Biomaterials and Nanomedicine, Barcelona, Spain
[3] Institute for Biomedical Image Analysis, UMIT, Hall in Tirol, Austria
[4] CETIR Grup Mèdic, Barcelona, Spain
[6] Institute of Anatomy & Musculoskeletal Research, PMU, Salzburg, Austria
[7] Musculoskeletal and Quantitative Imaging Research Group, University of California, San Francisco, CA, USA
[8] Department of Mechanical Engineering, University of Sheffield, Sheffield, UK

ABSTRACT

Femoral strength is estimated in clinical routine from 2D Dual-energy X-rays Absorptiometry (DXA). In this study, a new pipeline for femoral strength prediction from DXA images is presented, using a 3D reconstruction method of the shape and the Bone Mineral Density (BMD) distribution and a regression analysis based on partial least squares. A database of 90 proximal femoral cadaveric specimens, that were previously imaged and tested to measure their fracture load, was used to develop and to validate the method. The proposed pipeline resulted in a correlation coefficient of 0.85 between predicted and measured fracture load, while a regression using 2D BMD measurements from DXA resulted in a correlation coefficient of 0.77. With an improved femoral strength prediction from DXA images, this method opens interesting translational perspectives in clinics for a better diagnosis of osteoporosis and fracture risk prediction.

Index Terms— Statistical Model, 3D Reconstruction, Partial Least Square Regression, Femoral strength, Osteoporosis

1. INTRODUCTION

Due to the increasing life expectancy, the World Health Organization (WHO) estimated that the number of osteoporotic femoral fractures in the world will increase up to 40% by 2025 [1]. The diagnosis of osteoporosis and the prevention of femoral fracture is thus a major challenge for our society.

The relationship between bone strength and fracture risk is well established [2]. In clinical routine, the bone strength is estimated by measuring the areal Bone Mineral Density (aBMD, the bone mineral content divided by the projected area of the region of interest) using Dual-energy X-ray Absorptiometry (DXA) [3]. However, the two-dimensional (2D) measurement of the aBMD provides a partial description of the bone strength while a three-dimensional (3D) representation of the bone shape and Bone Mineral Density (BMD) distribution ensures an improved prediction of the femoral strength [4].

An accurate 3D representation of the femoral structure can be achieved using Quantitative Computed Tomography (QCT). A calibration phantom used during the CT-scan acquisition allows the conversion of the Hounsfield Units in the CT image to density values, leading to "quantitative" images of bone density. Different approaches were introduced to predict the femoral strength from such 3D QCT representations. Some studies proposed to compute geometrical and structural parameters (such as the neck-shaft angle, volumetric BMD and cross sectional area) from 3D QCT images and established statistical correlations between the parameters and the femoral strength [5, 6]. Finite element models have also been used to mechanically describe the femoral strength [7, 8]. However, such models are computationally very expensive, which complicates their use for clinical routine applications. Other approaches proposed to predict the femoral strength using statistical descriptions of the femoral shape and BMD based on Principal Component Analysis (PCA) [4]. These studies take profit of a full and detailed 3D representation of the femoral shape and BMD distribution to provide an improved estimation of the femoral strength. However, all these methods are based on the same imaging technique, QCT, which is a modality associated with high financial costs and a high radiation dose for the patient. Consequently, this imaging technique is currently not used for clinical routine assessment of femoral strength and follow-up of osteoporosis [9].

Therefore, we recently proposed a reconstruction method [10, 11] providing a 3D subject-specific modeling of the femoral bone from routinely-used 2D DXA images. This method uses a statistical model incorporating both the shape and the BMD distribution together with an intensity-based registration method to obtain 3D subject-specific reconstructions of the shape and BMD distribution of the femur. However, the ability of this technique to provide a better description of the femoral strength has not been evaluated yet.

In this study, we propose a new pipeline for femoral strength prediction from 2D DXA images. The method was evaluated on a large dataset of 90 femur specimens that were previously imaged and experimentally tested to measure their fracture load [12]. Using the reconstruction method as described in [10, 11], 3D shape and BMD distribution models were obtained for the 90 specimens. Multi-linear and Partial Least Squares (PLS) regressions [13] were used to establish statistical relationships between the shape and BMD descriptors, and the measured fracture load, resulting in the femoral strength prediction pipeline. The method was evaluated on the same set of 90 specimens in a leave-one-out cross validation.

2. METHOD

2.1 Data

90 proximal femur specimens (33 from male and 57 from female subjects with a mean age of 79±11 years) were included in this study to develop and validate the femoral strength prediction method. The samples were previously obtained from the Institute of Anatomy at the Ludwig Maximilians University Munich (Germany). They were prepared and scanned by using a 16-row MSCT scanner Sensation 16 (Siemens Medical Solutions, Erlangen, Germany). Afterwards, the femora were tested in a side impact configuration simulation of a sideways fall on the greater trochanter to measure the fracture load (for more details about the experiment, please refer to [12]).

The DXA images were not available for these specimens. Therefore simulated DXA images were generated from the QCT volumes using a ray-casting technique [14]. This ray-casting technique performs a parallel projection of the QCT volumes and has shown its ability to provide realistic DXA images [15].

2.2. 3D reconstruction from DXA image

The first step is to obtain 3D reconstructions of the shape and the BMD distribution from the (simulated) DXA of the 90 femur specimens. The 3D reconstruction method is summed-up in this section (for more details, please refer to [11]). First of all, a statistical model is built from a database of QCT of femurs. Using 3D/3D intensity-based registration methods, a point-to-point correspondence is established between all the femoral shapes and a voxel-to-voxel correspondence is found between the QCT density values. PCA is used to extract the principal modes of variation in terms of shape and BMD (Figure 1, left). This statistical model is subsequently used to recover a 3D reconstruction from a single 2D DXA image. In a 3D/2D intensity based-registration process, the statistical model parameters (pose, scale, shape parameters and BMD parameters) are optimized to maximize the similarity between the DXA image and Digitally Reconstructed Radiograph (DRR) generated form the projection of the model (Figure 1, right). This results in a 3D subject-specific reconstruction of the femur represented by a surface mesh and a volume of voxels for the BMD distribution. This method was evaluated *in vitro* [10] and *in vivo* [11] with a mean shape accuracy of respectively 1.2mm and 1.1mm and errors in terms of BMD distribution of 4.6% and 4.9%.

2.3. Femoral shape and density instances

The resulting 3D reconstructions present characteristics that prevent us to use them directly in our regression analysis: the reconstructed shapes and BMD distributions are not aligned onto a common reference and the BMD distributions do not have a voxel-to-voxel correspondence.

The parameters of the 3D reconstructions (pose, scale, shape parameters and BMD parameters) describe the deviation of the subject-specific model with respect to the mean instance of the statistical model. Using the subject-specific shape parameters, the shape instance corresponding to each of the specimens is generated. Then, the shape instances were scaled (using the scale parameter associated with each of the subject-specific models). This results in a set of shapes representing the deviation from the mean instance of the statistical model (Figure 2). In the same way, using the subject-specific BMD parameters, the density instance corresponding to each of the specimens was generated. Thanks to the properties of the statistical model, these density models are all instantiated over the mean shape statistical model, with a voxel-to-voxel correspondence between the instances.

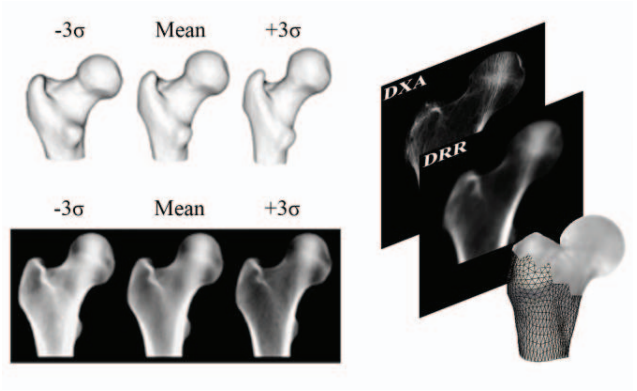


Figure 1: (left) Statistical model. First mode of variation (±3 standard deviations σ from the mean) for the shape and the 3D BMD distribution (frontal projection). (right) 3D reconstruction achieved by maximizing the similarity between a DRR generated from the statistical model and the DXA image.

Finally, the shapes are decimated and the volumes resampled to reduce their number of vertices and voxels, respectively, while keeping a point-to-point and a voxel-to-voxel correspondence between each sample (Figure 2).

2.4. Regression analysis

PLS regression is used to perform a regression analysis where the shapes vertices and the BMD distribution values are two separated sets of predictors and the fracture load the variable to be estimated (Figure 2). PLS regression combines features from PCA and multiple regression to find among the predictors $\mathbf{X}$ the set of components (called "latent vectors") that best describes both the predictors and the variables to be predicted. The independent predictors are decomposed as:

$$\mathbf{X} = \mathbf{T}\mathbf{P}^{\mathbf{T}} \quad (1)$$

where, by analogy with PCA, $\mathbf{T}$ is called the score matrix and $\mathbf{P}$ the loading matrix whose columns are the latent vectors [13]. The optimal number of latent vectors $\mathbf{P}$ to be used in the regression model was chosen as described in the following section 2.5.

Finally, a multi-linear regression was performed between the measured fracture load (variable to be predicted) and the latent vectors from the PLS regression ($\mathbf{P}_{\mathbf{Shape}}$ and $\mathbf{P}_{\mathbf{BMD}}$, equation 1) and the scale $\mathbf{S}$ of the shapes (from the previously computed similarity alignment) as the predictors, resulting in a fracture load estimated as:

$$\hat{\mathbf{F}} = (\mathbf{P}_{\mathbf{Shape}}, \mathbf{P}_{\mathbf{BMD}})\boldsymbol{\beta} + \mathbf{b}_{\mathbf{o}} \quad (2)$$

where $\boldsymbol{\beta}$ is the coefficients of the regression and $\mathbf{b}_{\mathbf{o}}$ the intercept.

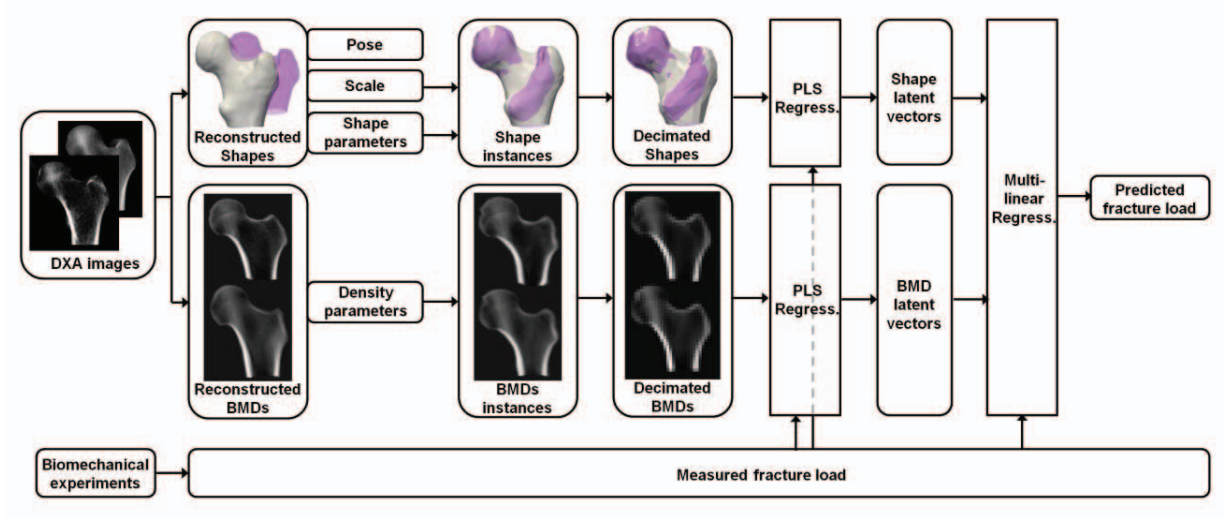


Figure 2: Femoral strength prediction pipeline

2.5. Method evaluation

The pipeline for femoral strength prediction was trained and evaluated using the database of 90 proximal femurs, by using a leave-one-out cross validation. That is, for each of the proximal femora, the whole regression analysis was performed on the 89 remaining specimens. The resulting regression matrices were then used to predict the fracture load of the femur that was removed from the database. The quality of the regression was evaluated by comparing the agreement between the predicted fracture load and the measured fracture load.

To choose the number of latent vectors to be used in the PLS regressions, the whole pipeline was tested by using the m first latent vectors resulting from the decomposition of the shape vertices and the n first latent vectors corresponding to of the BMD values, with m and n varying between 1 and 20. The combination resulting in the best estimation of the fracture load was chosen.

In clinical routine, physicians are used to base their diagnosis on the areal BMD value (aBMD) measured in the 2D DXA image at the femoral neck. Although the true DXA images of these specimens were not available, these values were previously measured and available for our study. A linear regression was thus computed between the measured fracture loads and the aBMD values of the femoral neck, in order to compare the accuracy of our femoral strength prediction pipeline to the clinical routine practices.

3. RESULTS

The search for the optimal number of latent vectors to be used in the PLS regression resulted in $m=10$ (shape latent vectors) and $n=3$ (BMD latent vectors). The evaluation of the whole regression pipeline resulted in a correlation coefficient of 0.85 between predicted and measured fracture load while the linear regression using the femoral neck aBMD resulted in a correlation coefficient of 0.77 (Figure 3), both associated with p-values < 0.005. The mean of the absolute differences between the predicted and measured fracture load was 577N using the proposed pipeline and 677N using the femoral neck (Table 1).

4. DISCUSSION

This study proposed and evaluated an entire pipeline predicting the femoral strength from a 2D DXA image, using a 3D reconstruction method [11] and a regression analysis. The method was found to be accurate (R=0.85), in comparison with an estimation from the aBMD of the femoral neck (R=0.77). This demonstrates that the 3D reconstruction recovered from the 2D DXA image provides a more accurate description of the femoral strength than the aBMD alone. This also shows that the combination of PLS and the multi-linear regression was an appropriate choice to reduce the (high) dimensionality of the system while providing an accurate statistical prediction.

By using a shape and density statistical model and a regression analysis, Schuler et al. [4] proposed a femoral fracture load prediction pipeline associated with a correlation coefficient of R=0.91. The method, however, requires QCT acquisitions as an input, whereas our method only uses the low radiation DXA images used in clinical routine.

The current method was tested using simulated DXA images from QCT, which constitutes the main limitation of this study. However, the simulation technique [15] already demonstrated its ability to generate realistic DXA images from QCT. We expect that a study from real DXA images would therefore not lead to very different results.

5. CONCLUSION

In this paper, a new femoral strength prediction pipeline from DXA images was introduced. The method provided an improved estimation of the fracture load (R=0.85) from a modality commonly used in clinics for the diagnosis of osteoporosis. Our future work aims at conducting an *in vivo* evaluation of the proposed pipeline, to evaluate its ability to provide an improved prediction of the fracture risk for osteoporotic patients.

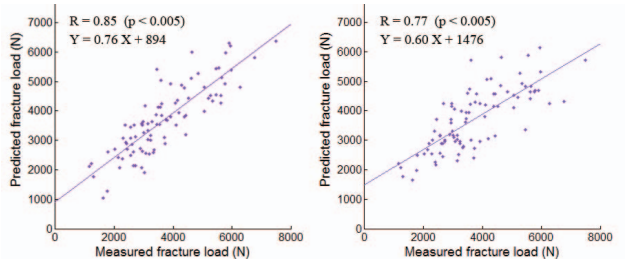


Figure 3: Linear correlation between the measured fracture load and the fracture load predicted from the whole pipeline (left) and directly predicted from the 2D aBMD of the femoral neck (right)

Table 1: Differences between the predicted and the measured fracture load (N)

	Mean ± 2StD*	Mean abs*	Max*
Proposed pipeline	1.8 ± 1404	577	1960
From 2D aBMD	1.0 ± 1710	677	2459

*Mean (systematic bias) ± 2StD (given a 95% confidence interval around the mean), Mean of the absolute differences, Maximum of the absolute differences

6. ACKNOWLEDGMENT

The research leading to these results has received funding from: the European Union Seventh Framework Programme (FP7/2007-2013) under grant agreement nr 269909, MySPINE project; the ERDF Operational Programme of Catalonia 2007-2013, through the 3D-FemOs project (exp. VALTEC 09-02-0012); the Spanish Ministry Science and Innovation (ref. TIN2009-14536-C02-01), Plan E and ERDF funds; a grant from the "Deutsche Forschungsgemeinschaft" (LO 730 / 3-1). The work of Alejandro Frangi is partially funded by the ICREA-Academia programme. The work of Tristan Whitmarsh is supported by the sub-programme PFIS (Ayudas predoctorales de formación en investigación en salud), an initiative funded by Acción Estratégica de Salud in the National R&D&i Plan 2008-2011 and financed by the Instituto de Salud Carlos III. The authors acknowledge Benedikt Schuler (Institute for Biomedical Image Analysis, UMIT, Hall in Tirol, Austria) and Dr. E. M. Lochmüller (Universitäts-Frauenklinik der LMU, Munich, Germany) for the data collection.

7. REFERENCES

[1] WHO, *Prevention and Management of Osteoporosis,* World Health Organization Technical Report Series 921, 2003.

[2] L. J. Melton, 3rd, E. J. Atkinson, W. M. O'Fallon, H. W. Wahner, and B. L. Riggs, "Long-term fracture prediction by bone mineral assessed at different skeletal sites," *J Bone Miner Res,* vol. 8, no. 10, pp. 1227-33, Oct, 1993.

[3] A. El Maghraoui, and C. Roux, "DXA scanning in clinical practice," *QJM,* vol. 101, no. 8, pp. 605-17, Aug, 2008.

[4] B. Schuler, K. D. Fritscher, V. Kuhn, F. Eckstein, T. M. Link, and R. Schubert, "Assessment of the individual fracture risk of the proximal femur by using statistical appearance models," *Med Phys,* vol. 37, no. 6, pp. 2560-71, Jun, 2010.

[5] V. Bousson, A. Le Bras, F. Roqueplan, Y. Kang, D. Mitton, S. Kolta, C. Bergot, W. Skalli, E. Vicaut, W. Kalender, K. Engelke, and J. D. Laredo, "Volumetric quantitative computed tomography of the proximal femur: relationships linking geometric and densitometric variables to bone strength. Role for compact bone," *Osteoporos Int,* vol. 17, no. 6, pp. 855-64, 2006.

[6] T. F. Lang, J. H. Keyak, M. W. Heitz, P. Augat, Y. Lu, A. Mathur, and H. K. Genant, "Volumetric quantitative computed tomography of the proximal femur: precision and relation to bone strength," *Bone,* vol. 21, no. 1, pp. 101-8, Jul, 1997.

[7] J. H. Keyak, "Improved prediction of proximal femoral fracture load using nonlinear finite element models," *Med Eng Phys,* vol. 23, no. 3, pp. 165-73, Apr, 2001.

[8] M. Bessho, I. Ohnishi, J. Matsuyama, T. Matsumoto, K. Imai, and K. Nakamura, "Prediction of strength and strain of the proximal femur by a CT-based finite element method," *J Biomech,* vol. 40, no. 8, pp. 1745-53, 2007.

[9] K. Engelke, J. E. Adams, G. Armbrecht, P. Augat, C. E. Bogado, M. L. Bouxsein, D. Felsenberg, M. Ito, S. Prevrhal, D. B. Hans, and E. M. Lewiecki, "Clinical use of quantitative computed tomography and peripheral quantitative computed tomography in the management of osteoporosis in adults: the 2007 ISCD Official Positions," *J Clin Densitom,* vol. 11, no. 1, pp. 123-62, Jan-Mar, 2008.

[10] T. Whitmarsh, L. Humbert, M. De Craene, L. M. d. R. Barquero, K. Fritscher, R. Schubert, F. Eckstein, T. Link, and A. F. Frangi, "3D bone mineral density distribution and shape reconstruction of the proximal femur from a single simulated DXA image: an in vitro study," in *SPIE Medical Imaging: Image Processing*, 2010, pp. 76234U-9.

[11] T. Whitmarsh, L. Humbert, M. De Craene, L. Del Rio Barquero, and A. Frangi, "Reconstructing the 3D Shape and Bone Mineral Density Distribution of the Proximal Femur from Dual-energy X-ray Absorptiometry," *IEEE Trans Med Imaging*, Jul 29, 2011.

[12] F. Eckstein, C. Wunderer, H. Boehm, V. Kuhn, M. Priemel, T. M. Link, and E. M. Lochmuller, "Reproducibility and side differences of mechanical tests for determining the structural strength of the proximal femur," *J Bone Miner Res,* vol. 19, no. 3, pp. 379-85, Mar, 2004.

[13] H. Abdi, "Partial least squares regression and projection on latent structure regression (PLS Regression)," *Wiley Interdisciplinary Reviews: Computational Statistics,* vol. 2, no. 1, pp. 97-106, 2010.

[14] A. J. Burghardt, G. J. Kazakia, T. M. Link, and S. Majumdar, "Automated simulation of areal bone mineral density assessment in the distal radius from high-resolution peripheral quantitative computed tomography," *Osteoporos Int,* vol. 20, no. 12, pp. 2017-24, Dec, 2009.

[15] B. C. Khoo, K. Brown, C. Cann, K. Zhu, S. Henzell, V. Low, S. Gustafsson, R. I. Price, and R. L. Prince, "Comparison of QCT-derived and DXA-derived areal bone mineral density and T scores," *Osteoporos Int,* vol. 20, no. 9, pp. 1539-45, Sep, 2009.